Impact of cystinosin glycosylation on protein stability by differential dynamic SILAC

Nathalie Névo, Lucie Thomas, Cerina Chhuon, Zuzanna Andrzejewska, Joanna Lipecka, François Guillonneau, Anne Bailleux, Aleksander Edelman, Corinne Antignac, Ida Chiara Guerrera

▶ **To cite this version:**

Nathalie Névo, Lucie Thomas, Cerina Chhuon, Zuzanna Andrzejewska, Joanna Lipecka, et al.. Impact of cystinosin glycosylation on protein stability by differential dynamic SILAC. Molecular and Cellular Proteomics, 2017, 16 (3), pp.457-468. 10.1074/mcp.M116.063867 . inserm-01438319

HAL Id: inserm-01438319

https://inserm.hal.science/inserm-01438319v1

Submitted on 17 Jan 2017

HAL is a multi-disciplinary open access archive for the deposit and dissemination of scientific research documents, whether they are published or not. The documents may come from teaching and research institutions in France or abroad, or from public or private research centers.

L'archive ouverte pluridisciplinaire **HAL**, est destinée au dépôt et à la diffusion de documents scientifiques de niveau recherche, publiés ou non, émanant des établissements d'enseignement et de recherche français ou étrangers, des laboratoires publics ou privés.

MCP Papers in Press. Published on January 12, 2017 as Manuscript M116.063867

Impact of cystinosin glycosylation on protein stability by differential dynamic SILAC

Nathalie Nevo [1,6]*, Lucie Thomas [1,6]*, Cerina Chhuon [2,6], Zuzanna Andrzejewska [1,6], Joanna Lipecka [3,6], François Guillonneau [4,6], Anne Bailleux [1,6], Aleksander Edelman [2,5], Corinne Antignac [1,6,7], Ida Chiara Guerrera [2,6]

[1]INSERM U1163, Laboratory of Hereditary Kidney Diseases, Imagine Institute, Paris, France

[2]Plateforme Protéomique Paris Descartes Necker, PPN, 3P5-Necker, SFR Necker, US24, 75014 Paris, France

[3]The CPN Proteomics Facility – 3P5, Center of Psychiatry and Neuroscience, UMR INSERM 894, 75014 Paris, France

[4]Plateforme Protéomique Paris Descartes Cochin, 3P5-Cochin, 75014 Paris, France

[5] INSERM U1151, 75015 Paris, France

[6]Paris Descartes-Sorbonne Paris Cité University, Paris, France

[7]Assistance Publique - Hôpitaux de Paris (AP-HP), Department of Genetics, Necker Hospital, Paris, France.

*These authors contributed equally to the work.

Running title: Cystinosin turnover.

Corresponding Author:

Ida Chiara Guerrera,

Hôpital Necker, site Broussais

14 Rue Maria Helena Vieira Da Silva

75993 Paris cedex 14

Tel: 01 72 60 63 31

Email: chiara.guerrera@inserm.fr

ABBREVIATIONS

AA: amino acids

Endo H: Endoglycosidase H

ER: endoplasmic reticulum

FDR: false discovery rate

Copyright 2017 by The American Society for Biochemistry and Molecular Biology, Inc.

ASBMB MOLECULAR & CELLULAR PROTEOMICS MCP

ASBMB MOLECULAR & CELLULAR PROTEOMICS MCP

LFQ: label-free quantification

MS: mass spectrometry

PDI: protein disulfide isomerase

PNGase F: Peptide:N-glycosidase F enzyme

RIA: relative isotope abundance

RSLC: rapid separation liquid chromatography

SILAC: stable isotope labelling by amino acids in cell culture

TM: transmembrane

WT: wild-type

ASBMB MOLECULAR & CELLULAR PROTEOMICS MCP

SUMMARY

Cystinosis is a rare autosomal recessive lysosomal storage disorder characterized by intralysosomal accumulation of cystine. The causative gene for cystinosis is *CTNS*, which encodes the protein cystinosin, a lysosomal proton-driven cystine transporter. Over 100 mutations have been reported, leading to varying disease severity, often in correlation with residual cystinosin activity as a transporter and with maintenance of its protein-protein interactions.

In this study, we focus on the ΔITILELP mutation, the only mutation reported that sometimes leads to severe forms, inconsistent with its residual transported activity. ΔITILELP is a deletion that eliminates a consensus site on N66, one of the protein's seven glycosylation sites. Our hypothesis was that the ΔITILELP mutant is less stable and undergoes faster degradation.

Our dynamic SILAC study clearly showed that wild-type cystinosin is very stable, while ΔITILELP is degraded three times more rapidly. Additional lysosome inhibition experiments confirmed ΔITILELP instability and showed that the degradation was mainly lysosomal. We observed that in the lysosome, ΔITILELP is still capable of interacting with the V-ATPase complex and some members of the mTOR pathway, similar to the wild-type protein. Intriguingly, our interactomic and immunofluorescence studies showed that ΔITILELP is partially retained at the endoplasmic reticulum (ER). We proposed that the ΔITILELP mutation causes protein misfolding, ER retention and inability to be processed in the Golgi apparatus, and we demonstrated that ΔITILELP carries high-mannose glycans on all six of its remaining glycosylation sites. We found that the high turnover of ΔITILELP, due to its immature glycosylation state in combination with low transport activity, might be responsible for the phenotype observed in some patients.

Data are available via ProteomeXchange with identifier PXD004948, PXD005357 and on Panorama Public at https://panoramaweb.org/labkey/Guerrera.url.

ASBMB MOLECULAR & CELLULAR PROTEOMICS MCP

INTRODUCTION

Cystinosis (OMIM 219800) is a rare autosomal recessive lysosomal storage disorder characterized by intralysosomal accumulation of cystine, leading to impaired function of multiple organs (1). Based on the age of onset and severity of symptoms, three clinical forms of cystinosis have been described: infantile (severe), juvenile and ocular (mild).

The causative gene for cystinosis is *CTNS*, which encodes the protein cystinosin, a lysosomal proton-driven cystine transporter (2,3,4). Recently, we have shown that in addition to transporting cystine, cystinosin is involved in nutrient-sensing in kidney proximal tubular cells via interactions with v-ATPase, Ragulator and Rags (5), and that the lack of cystinosin results in dysregulation of the mTOR signaling pathway.

Cystinosin is a 367-amino-acid (AA) protein with a nominal mass of 41.7 kDa. It has a short cytosolic 10-AA C-terminal tail, seven transmembrane (TM) domains spanning the lysosomal membrane and a 128-AA N-terminal region in the lysosomal lumen bearing seven N-glycosylation consensus sites N-X-S/T (N36, N41, N51, N66, N84, N104 and N107, hereafter referred to as N1 to N7) (Figure 1A). The molecular weight (MW) of mature cystinosin is estimated at approximately 56 kDa. Cystinosin contains two lysosomal targeting motifs: a classical tyrosine-based motif (GYDQL) in the C-terminal tail and a conformational signal located on the fifth inter-TM loop (3, 6).

Most early functional studies conducted on a set of 31 cystinotic mutations revealed a correlation between cystine transport activity and severity of symptoms (4). Most infantile mutations abolished cystine transport, whereas less severe mutations only reduced it (4). Patients affected by severe symptoms harbor severe mutations on both alleles, while patients with milder forms usually carry non-severe mutations on both alleles or in association with a severe mutation.

ASBMB MOLECULAR & CELLULAR PROTEOMICS MCP

However, some discrepancies have been observed, such as with I67-P73del (ΔITILELP), which leads to 19% residual transport activity and is considered a non-severe mutation (4). Individuals with the ΔITILELP mutation on both alleles have the juvenile form, whereas those with the ΔITILELP mutation on one allele in association with the 57 kb deletion (the most common severe mutation) can develop the infantile form (7–9). ΔITILELP is an in-frame deletion adjacent to an N-glycosylation site at position 66. The ΔITILELP mutation (deletion of AA67-73) is predicted to prevent the recognition consensus sequence of N-glycosylation N-X-S/T on NIT (AA66-68) by oligosaccaryltransferase. Therefore, ΔITILELP results in the removal of seven amino acids in the N-terminal luminal region and the loss of glycosylation on N66, the fourth of seven N-glycosylation sites (10). To date, ΔITILELP is the only mutation detected in patients that leads to faulty glycosylation.

As glycosylation of lysosomal membrane proteins is known to protect from proteolysis (11), we hypothesized that faulty glycosylation caused by ΔITILELP might influence the stability of the protein. To investigate the stability of ΔITILELP, we compared its degradation rate to wild-type (WT) cystinosin. As additional controls, we also studied the degradation of two mutations that do not impact glycosylation sites (N288K and N323K). The classical approach for protein-turnover studies is pulse-chase labeling with radioactive amino acids. We used an alternative approach based on mass spectrometry, known as dynamic stable isotope-labeling by amino acids in cell culture (dynamic SILAC) (12, 13). In this metabolic-labeling time-course experiment, the ratio of the unlabeled and labeled peptides of a protein reflects the ratio of pre-existing and newly synthesized proteins at each measured time point. It has been shown that from these values, the degradation rate of the proteins can be successfully calculated by curve-plotting or mathematical formulas (14, 12).

ASBMB MOLECULAR & CELLULAR PROTEOMICS MCP

To expand our knowledge of the cellular mechanisms involved in the pathogenicity of ΔITILELP, we analyzed its fate in the cell by studying its glycosylation, cellular localization and specific protein partners, as compared to WT cystinosin.

EXPERIMENTAL PROCEDURES

Antibodies

Antibodies were obtained from the following sources: antibody to PDI and calnexin from Enzo Life Sciences, antibody to GFP from Roche, anti-mouse IgG-HRP from GE Healthcare, and Alexa Fluor 555- and 647-conjugated secondary antibodies from Life Technologies. The Lamp-1 (1D4B) monoclonal antibody developed by J. Thomas August was obtained from the Developmental Studies Hybridoma Bank, developed under the auspices of the National Institute of Child Health and Human Development, and maintained by the Department of Biology at the University of Iowa, Iowa City, Iowa, USA.

Cell culture

NIH/3T3 fibroblast cell lines were grown in DMEM supplemented with 10% foetal bovine serum (FBS), 100 U/mL penicillin, 0.1 mg/mL streptomycin and 2 mM L-glutamine (complete DMEM medium) (all from Life Technologies).

For dynamic SILAC studies, NIH/3T3 cells stably expressing different fusion proteins were plated at 4×10^6 cells per 150-mm cell-culture dish. After removing the complete DMEM medium, the cells were quickly washed twice with PBS and then incubated with DMEM medium lacking arginine and lysine, supplemented with 175.2 mg/l [$^{13}C_6$] L-arginine, 84 mg/l [$^{13}C_6$] L-lysine, 10% dialysed FBS (all from ThermoFisher), 100 mg/L proline (Sigma-Aldrich), 100 U/mL penicillin, 0.1 mg/mL streptomycin and 2 mM L-glutamine for chase periods of 0, 6, 18 and 24 h. At these times, the cells were treated for immunoprecipitation before being processed for proteomic turnover analysis.

ASBMB
MOLECULAR & CELLULAR PROTEOMICS
MCP

To calculate the cell-growth rate (D), WT and mutant cells were plated in 10-cm tissue-culture dishes at 1.3×10^6 cells per 150-mm cell-culture dish, cultivated for 24 h, collected at several time-points (0, 6, 18 and 24 h) and then counted using the Beckman Coulter Z2 cell counter. The cell growth rate (D) was calculated by fitting the number of cells (*y*) at different times (*x*) to an exponential growth curve in Microsoft Excel, using the formula: $y = a * eDx$, where "a" is the number of cells at 0 h.

Generation of stable cell lines

To generate NIH/3T3 fibroblast cell lines stably expressing human protein cystinosin-EGFP, the construct pCTNS-EGFP (3) was sub-cloned into the lentiviral pRRL.SIN.cPPT.PGK/WPRE vector (15). The cystinosin mutants ΔITILELP, N288K, N323K (5) and N1N7 (the seven putative N-glycosylated sites mutated in alanine) were obtained by the modification of the pRRL.SIN.cPPT.PGK/WPRE-CTNS-EGFP construct with specific mutagenic primers using the Stratagene QuikChange® Site-Directed Mutagenesis Kit according to the manufacturer's recommendations. Lentiviruses were produced in HEK293T cells as previously described (5). NIH/3T3 cells were transduced by lentiviral particles containing CTNS-EGFP or its mutated forms at an MOI of 7 in the presence of 8 µg/mL polybrene.

Generation of EGFP fusion constructs and transfection of NIH/3T3 fibroblasts

The pCTNS-EGFP construct and its mutant form ΔITILELP have been described previously (3). For the mutant N66A (the N66 glycosylation site mutated in alanine), the modification of the pCTNS-EGFP construct (3) was carried out using the Stratagene QuikChange Site-Directed Mutagenesis Kit according to the manufacturer's recommendations. NIH/3T3 fibroblasts were transfected with 2 µg of the different constructs using Lipofectamine® 2000 reagent (Invitrogen) according to the manufacturer's protocol. Cells were lysed 48 h after transfection for western blotting.

Co-immunoprecipitation and immunoblotting

ASBMB MOLECULAR & CELLULAR PROTEOMICS MCP

Co-immunoprecipitation and western blotting experiments on cystinosin-EGFP and its mutants in NIH/3T3 cells were performed as previously described (5). Immunoprecipitated calnexin was expressed as a ratio of the signals of calnexin and cystinosin-EGFP using BIO-1D software (Vilber Lourmat). Statistical analysis using the Kruskal-Wallis test ($p<0.05$) with post-hoc Dunn's test was performed with Prism version 5 (GraphPad software). The threshold for statistical significance was set at $p<0.05$. Each bar represents the mean ± SEM from four independent experiments.

Immunofluorescence

NIH/3T3 cells were plated on glass coverslips in 12-well tissue-culture dishes, then 24–38 hours later were treated as previously described (5). For the colocalization analysis, the reticular and lysosomal compartments were defined by delimiting the PDI- or Lamp1-labeled areas, respectively, using ImageJ 1.50 software. The reticular or lysosomal accumulation of cystinosin-EGFP or its mutants was measured as a ratio, expressed in percentage of GFP fusion proteins that colocalized with the PDI- or Lamp1-labeled areas. Statistical analysis using the Kruskal-Wallis test with post-hoc Dunn's test was performed with Prism version 5 (GraphPad software). The threshold for statistical significance was set at $p<0.05$. Three independent biological replicates were analyzed, and for each experiment, colocalization GFP:PDI or GFP:Lamp1 for five cells of each cell type was performed.

PNGase F and Endo H treatments

Cell lysates were treated for 1 h at 37°C with 100 U of PNGase F or Endo H (BioLabs) per µg of total proteins according to the manufacturer's recommendations except for the denaturation step, which was done at 50°C instead of 100°C. The resulting cell lysates were analysed by western blotting.

Drug treatment and FACS analysis

NIH/3T3 cells stably expressing WT cystinosin-EGFP and ΔITILELP-EGFP were incubated with 10 µM clasto-lactacystin β-lactone (Calbiochem) or 100 nM bafilomycin A1 (SIGMA) for 24 h in the complete

ASBMB MOLECULAR & CELLULAR PROTEOMICS MCP

DMEM medium. Cells were then harvested by using trypsin, and centrifuged for 2.5 min at 1500 rpm. The cell pellets were washed once with PBS and resuspended in 500 µl PBS with 1% bovine serum albumin. EGFP expression was analyzed by direct flow cytometry using FACSCalibur with CellQuest software (BD Biosciences). Dead cells and debris were excluded by gating on forward/side light scatter, and 10,000 events corresponding to EGFP-positive cells were analyzed per sample. The average expression level of EGFP in individual NIH/3T3 cells was determined by calculating the geomean fluorescence intensity (GFI). The GFIs of the treated cells were normalized relative to the GFI of the untreated cells (with DMSO vehicle). Statistical analysis using the Kruskal-Wallis test with post-hoc Dunn's test was performed with Prism Version 5 (GraphPad software). The threshold for statistical significance was set at $p<0.05$. Each bar represents the mean ± SEM from five independent experiments.

Mass spectrometry (MS) analysis for turnover study

For turnover studies, immunoprecipitated protein samples were resolved by SDS-PAGE on 10% gel and large protein bands corresponding to cystinosin were excised. In-gel trypsin digestion was performed as previously described (5). Nano-LC-MS/MS analysis of in-gel digested samples was performed on an Ultimate 3000 Rapid Separation Liquid Chromatography (RSLC) system coupled to a Q-Exactive Plus mass spectrometer (Thermo Scientific, Waltham, MA, USA). Extracted peptides were resuspended in 0.1% (v/v) trifluoroacetic acid and 10% acetonitrile, then loaded onto a µ-precolumn (Acclaim PepMap 100 C18, cartridge, 300 µm i.d.×5 mm, 5 µm, Dionex), followed by separation on the analytical 50-cm nano column (0.075 mm ID, Acclaim PepMap 100, C18, 2 µm, Dionex). The chromatography solvents were (A) 0.1% formic acid in water, and (B) 80% acetonitrile with 0.08% formic acid. Peptides were eluted from the column using a gradient from 5% to 40% B over 38 min, then analyzed by data-dependent MS/MS, using the top-10 acquisition method. Briefly, the instrument settings were as follows: resolution was set to 70,000 for MS scans and 17,500 for the data-dependent MS/MS scans to increase speed. The MS AGC

target was set to 3.10^6 counts with a maximum injection time of 200 ms, while the MS/MS AGC target was set to 1.10^5 with a maximum injection time of 120 ms. Dynamic exclusion was set to 30 s.

Raw files were processed using the Proteome Discoverer 1.4.0.288 software (Thermo Scientific, San Jose, CA, USA) and searched using Mascot 2.2 against the *Mus musculus* Uniprot KB/Swiss-Prot database v.5/7/2012 (16,331 entries) integrated with the sequences of the EGFP cystinosin WTs and mutants. Search parameters included fixed modification with carbamidomethyl (C) and variable modifications with oxidation (M), Label:^{13}C(6) (K), Label:^{13}C(6) (R), and two missed cleavages. The enzyme was trypsin, monoisotopic peptide mass tolerance was ±2 ppm, and fragment mass tolerance was ±0.05 Da. The identification validation was performed using a percolator, allowing 1%–5% of target FDR for peptides based on the q-value and determined by the target-decoy approach.

The mass spectrometry proteomics data have been deposited at Panorama Public (https://panoramaweb.org/labkey/Guerrera.url). The MS raw files related to the turnover study have been deposited at the ProteomeXchange Consortium via the PRIDE (17) partner repository with the dataset identifier PXD005357.

Turnover data analysis

The loss of a protein can be calculated from the relative isotope abundance (RIA) at each time point. The RIA represents the portion of the residual pre-existing protein (MS1 area of the light peptides: A_L) versus the total amount of the protein in the cell, both pre-existing (A_L) and newly synthesized (MS1 area of the heavy peptides: A_H), at each time-point. RIA is therefore calculated as:

$$RIA_{L,t} = \frac{A_{L,t}}{A_{H,t} + A_{L,t}}$$

The MS1 areas A_H and A_L were extracted for peptides SVSLTVPPVVK, EDGNILGHK, FEGDTLVNR and FSVSGEGEGDATYGK for cystinosin-EGFP using Skyline v2.6.0 (freely available at

ASBMB MOLECULAR & CELLULAR PROTEOMICS MCP

ASBMB MOLECULAR & CELLULAR PROTEOMICS MCP

https://skyline.gs.washington.edu). To insure accuracy in the peak attribution, a dedicated Skyline library was built using the search files from the same samples. Peptide YFPQAYMNFYYK was excluded due to the presence of a methionine partially oxidised under different conditions. A thorough manual check and correction of peak picking was performed based on retention time and mass error. The $RIA_{L,t}$ was calculated for each peptide at each time-point (0, 6, 18 and 24 h) for WT cystinosin and each mutants ΔITILELP, N288K, N323K and N1N7 (deglycosylated form of cystinosin) (12, 16). The rate of loss of the protein, K_{loss}, was calculated fitting the $RIA_{L,t}$ to an exponential decay curve using Excel and GraphPad v7:

$$y = e^{-K_{loss}x}$$

K_{loss} was additionally calculated mathematically in Excel, as the average of the K_{loss} at each single time-point for each peptide (14, 16), in each independent biological triplicate:

$$K_{loss} = \frac{t * ln(\frac{A_H}{A_L} + 1)}{t^2}$$

The rate of degradation (K_{deg}) was calculated as the difference between the rate of loss (K_{loss}) and the cell-growth rate (D):

$$K_{deg} = K_{loss} - D$$

At least three independent biological replicates were analyzed (four for WT cystinosin-EGFP, three for ΔITILELP, N288K, N323K and N1N7). For each experiment, three to four peptides were measured at 0, 6, 18 and 24 h (details in Table S1). Each mutant was always run in parallel with WT cystinosin-EGFP. The cell-growth rate (D) was measured in at least two independent experiments for each sample (four for WT cystinosin-EGFP, two each for ΔITILELP, N323K, N288K and N1N7) (details in Table S3). Statistical analysis using one-way ANOVA was performed with Prism version 7 (GraphPad software), using K_{loss} values obtained by curve-fitting and formulas, from at least three independent experiments and three to four peptides per time-point. The threshold for statistical significance was set at $p<0.05$. Each bar represents the mean ± SD.

ASBMB MOLECULAR & CELLULAR PROTEOMICS MCP

Mass spectrometry analysis for interactomic study

For interactomic analysis, co-immunoprecipitated protein samples were concentrated on top of 10% SDS-PAGE gel and excised. In-gel trypsin digestion was performed as previously described (5). Analysis by LC-MS/MS was performed as described in "Mass spectrometry (MS) analysis for turnover study", except for gradient length, which was 120 min rather than 38 min. The mass spectrometry proteomics data and details on the identifications and quantifications have been deposited at the ProteomeXchange Consortium via the PRIDE (17) partner repository with the dataset identifier PXD004948.

Interactomic data analysis of the MS files was processed with MaxQuant software version 1.5.2.8 and searched with the Andromeda search engine against the *Mus musculus* Uniprot KB/Swiss-Prot database 2016_01 (20199 entries), integrated with FASTA sequences of WT cystinosin-EGFP. To search parent mass and fragment ions, we set initial mass deviations of 4.5 ppm and 20 ppm, respectively. The minimum peptide length was set at seven amino acids and strict specificity for trypsin cleavage was required, allowing up to two missed cleavage sites. Carbamidomethylation (Cys) was set as a fixed modification, whereas oxidation (Met) and N-terminal acetylation were set as variable modifications. Match-between-runs was allowed using default parameters. The false discovery rate (FDR) for PSM and protein identification was set to 1%, determined by a target-decoy approach. Scores were calculated in MaxQuant as previously described, and left as the default parameters (18). The reverse- and common-contaminant hits were removed from the MaxQuant output. Proteins were quantified according to the MaxQuant label-free algorithm using Label-free Quantification LFQ intensities (19). Protein quantification was obtained using at least two peptides per protein. For pathway analysis, we annotated all of the proteins according to the KEGG database, and selected those classified as "protein processing in endoplasmic reticulum".

ASBMB MOLECULAR & CELLULAR PROTEOMICS MCP

Three biological replicates were analyzed for WT cystinosin-EGFP, ΔITILELP-EGFP and controls (without GFP). Statistical analysis between WT cystinosin and ΔITILELP was performed after the filtering-out of all proteins identified the negative control with Perseus software (version 1.5.5.3, freely available at www.perseus-framework.org) (20). For statistical comparison, the LFQ data were transformed in log2 and imputed to fill in the missing data points by creating a Gaussian distribution of random numbers with a standard deviation of 33% relative to the standard deviation of the measured values, and a three-standard-deviation downshift of the mean to simulate the distribution of the low signal values. We performed a volcano plot analysis of the data using FDR=0.05 and S0=0.5.

Experimental design and statistical rationale

For the western blot analyses, we performed four independent experiments. Statistical analysis was done with the Kruskal-Wallis test with post-hoc Dunn's test (threshold $p<0.05$). For colocalization statistical analysis, we performed three independent biological replicates. Statistical analysis was done with Kruskal-Wallis and post-hoc Dunn's tests (threshold $p<0.05$). For drug treatments and FACS analyses, we performed five independent biological replicates. Statistical analysis was done with Kruskal-Wallis and post-hoc Dunn's tests (threshold $p<0.05$).

For MS turnover studies, we performed a minimum of three independent biological replicates (four for WT cystinosin-EGFP, three each for ΔITILELP, N288K, N323K and N1N7). For each experiment, three to four peptides were measured at 0, 6, 18 and 24 h (details in Table S1). Each mutant was always run in parallel with WT cystinosin-EGFP. The cell-growth rate (D) was measured in at least two independent experiments for each sample (four for WT cystinosin-EGFP, two each for ΔITILELP, N323K, N288K and N1N7) (details in Table S3). Statistical analysis using one-way ANOVA was performed with Prism version 7 (GraphPad software) using K_{loss} values obtained by a formula (threshold $p<0.05$) (details in Table S4a).

ASBMB MOLECULAR & CELLULAR PROTEOMICS MCP

For MS-based interactomic studies, we performed three independent biological replicates for WT cystinosin-EGFP, ΔITILELP-EGFP and controls (cells without GFP expressing plasmid). Statistical analysis between WT cystinosin and ΔITILELP was performed with Perseus software (version 1.5.0.31). For statistical comparison, the LFQ data were transformed in log2 and imputed to fill in the missing data points by creating a Gaussian distribution of random numbers with a standard deviation of 33% relative to the standard deviation of the measured values, and with two to five standard deviations downshift of the mean to simulate the distribution of the low signal values. We performed a volcano plot analysis based on the t test, applying FDR=0.05 and S0=1.

RESULTS

Detection of EGFP-tagged cystinosin peptides by MS

To analyze the turnover of WT and mutated cystinosin, we transduced 3T3 cells with lentiviral constructs to stably express the cystinosin-EGFP fusion protein and its mutated forms. The schematic representation of WT cystinosin and ΔITILELP can be found in Figure 1A and 1B. We consistently identified specific cystinosin peptides in accordance with the WT or the mutated forms N288K and N323K (Figure S1). In all analyzed forms of cystinosin, we could identify the peptide AA23-33 (SVSLTVPPVVK). These data suggest that the signal peptide of cystinosin was cleaved after S22, generating a new N-terminal sequence starting with SVSLTVPPVVK, despite previous reports describing an uncleavable signal peptide (3, 21). Our data agreed with the prediction of the currently used algorithm (http://www.cbs.dtu.dk/services/SignalP) (Figure S2).

ΔITILELP-EGFP mutation results in the loss of seven amino acids and one N-glycosylation site (N66); consequently, its expected molecular mass would be approximately 3 kDa smaller than that of WT cystinosin, if all remaining sites were fully glycosylated. However, the observed molecular mass of the glycosylated form was much lower than expected and inconsistent with the simple deletion of seven

ASBMB MOLECULAR & CELLULAR PROTEOMICS MCP

amino acids and the loss of one glycan (Figure 1C). Again, the detection of the peptide SVSLTVPPVVK (Figure 1B) for ΔITILELP indicated that the N-terminal domain of the mutated protein was intact.

To further verify the effect of the glycan in position 66 (N66) on the protein electrophoretic profile, we substituted the N-glycosylated site N66 with alanine (N66A). N66A showed a molecular mass shift compared to WT cystinosin that was consistent with the loss of one glycan (Figure 1C).

Half-life of cystinosin and ΔITILELP

To investigate whether N-glycosylation influences the stability of ΔITILELP, we measured protein degradation using a dynamic SILAC approach. We incubated unlabelled cells expressing cystinosin and ΔITILELP with [$^{13}C_6$] L-arginine and [$^{13}C_6$] L-lysine for 6, 18 and 24 h in order to selectively label newly synthesised proteins. The WT cystinosin was used as the main control while N288K and N323K, which do not impact glycosylation, were used as additional controls. An artificial mutant simulating the loss of the seven glycosylations (N1N7) was also investigated.

At each time-point, cystinosin and its mutants were immunoprecipitated and analyzed by LC-MS/MS. For each sample, the MS analysis was performed to confirm the presence of cystinosin or its mutants and to verify the incorporation of labelled amino acids during the time-course. For calculating the turnover rate of a given protein, we used the precursor ion signal (MS1 area) from four labelled and unlabelled peptides from that protein at each time-point (an example for one peptide is shown in Figure 2). The extracted MS1 areas were used to calculate the relative isotope abundance at each time point (RIA_t) for each cell type and each replicate (Table S1). RIA_L at time 0 was always set to 1 because the cells contained 100% of the light amino acids at this time-point. The K_{loss} values were obtained either by fitting (RIA_L , t) on an exponential decay curve (K_{loss} by formula) (12, 13, 16) or by single-time-point analysis (K_{loss} by fitting) (14, 16) (Table S2). The K_{loss} obtained with the two approaches fit a linear regression curve (R^2=0.985), suggesting that the K_{loss} values obtained by fitting on an exponential decay curve or on a

ASBMB MOLECULAR & CELLULAR PROTEOMICS MCP

single-time-point analysis are very similar to each other (Figure S3). The cells expressing cystinosin and its mutants were counted at each time-point to determine the cell-growth rate or dilution rate (D) (Table S3).

The reproducibility of the measurements reported on the exponential decay curves between three different independent biological replicates appeared to be very high (Figure 3) (16). The WT cystinosin was found to be very stable, with K_{loss}=0.0434±0.008, while ΔITILELP was degraded three times faster than WT cystinosin, with K_{loss}=0.1291±0.014 (Figure 3, Table S2). The division rates of cells overexpressing cystinosin-EGFP and ΔITILELP-EGFP were similar, indicating that the loss rate of ΔITILELP was due to increased degradation (Figure 3 histograms, Table S4). N288K and N323K showed a tendency, though not significant, toward increased degradation when compared to WT cystinosin. Strikingly, the substitution of seven asparagine residues with alanine residues (N1N7), mimicking complete deglycosylation, resulted in a very stable protein with a turnover similar to that of WT cystinosin (Figure 3).

Cystinosin and ΔITILELP lysosomal degradation

To confirm the higher degradation rate of ΔITILELP, fibroblasts expressing ΔITILELP-EGFP or cystinosin-EGFP were treated for 24 h with bafilomycin A1 (Baf A1), an activity-inhibitor of lysosomes and other acidic compartments. EGFP fluorescence was then measured by flow cytometry. Upon Baf A1 treatment, the EGFP signal was significantly increased for both WT cystinosin and ΔITILELP when compared to DMSO-treated cells (vehicle), indicating that both proteins undergo lysosomal degradation. To test whether the proteasome partially contributes to the degradation of ΔITILELP, the same fibroblasts were treated with clasto-lactacystin β-lactone (CL), a specific proteasome inhibitor. In the fibroblasts expressing cystinosin-EGFP or ΔITILELP-EGFP, the EGFP fluorescence intensity did not change after 24 h

ASBMB MOLECULAR & CELLULAR PROTEOMICS MCP

of CL treatment, suggesting that proteasome degradation does not contribute significantly to the increased loss of ΔITILELP (Figure 4).

ER retention of ΔITILELP

To investigate whether the ΔITILELP mutation impacts protein-protein interactions, we explored the interactome of ΔITILELP compared to that of WT cystinosin by MS. We compared proteins co-immunoprecipitated by WT cystinosin or by ΔITILELP, then identified 181 such proteins as potentially specific interactants of WT cystinosin and/or ΔITILELP, as they were not identified in the negative control (without GFP) (Table S5). The results of this MS analysis largely confirmed our previously published interaction network generated for WT cystinosin (5), as we identified eight subunits of the vacuolar type H^+-ATPase (V-ATPase) and Rag GTPase C (Figure 5, full protein list in Table S5). ΔITILELP maintained the same protein-protein interactions as WT cystinosin in the lysosome. However, ΔITILELP, but not WT cystinosin, specifically co-immunoprecipitated 17 proteins directly implicated in protein-processing in the ER (Figure 5).

We investigated the cellular distribution of WT cystinosin and its mutants in cells stably overexpressing EGFP-tagged proteins by immunofluorescence. WT cystinosin-EGFP presented a predominant co-localization with the late endosomal-lysosomal marker Lamp-1 (83.62±1.73%) and a minor co-localization with protein disulfide isomerase (PDI), an ER marker (15.64±2.28%). Similar to WT cystinosin, N288K and N323K showed predominant lysosomal localization in 3T3 cells. In striking contrast, the signal for ΔITILELP corresponding to an ER localization was higher (48.26±2.57%), along with a decreased punctuated late endosomal-lysosomal localization pattern (47.66±2.01%) (Figure 6A and 6B). Multitransmembrane proteins that do not acquire proper configurations accumulate in the ER, where they are recognized by calnexin (22). To analyze the interaction between cystinosin and this chaperone, lysates of 3T3 cells stably expressing cystinosin-EGFP or its mutated forms were immunoprecipitated

ASBMB MOLECULAR & CELLULAR PROTEOMICS MCP

with anti-GFP antibody, and co-immunoprecipitated endogenous calnexin was detected by western blotting. As expected from the localization data, interactions with calnexin were significantly increased for ΔITILELP compared to WT cystinosin, N288K or N323K (Figure 6C and 6D). The mutants N66A and N1N7 appeared to localize at the lysosome as well, without any ER retention (Figure S4). Together, these data indicate that the ΔITILELP mutation leads to partial retention of cystinosin in the ER due to misfolding of the protein.

N-linked high-mannose glycans of ΔITILELP

Lysosomal transmembrane proteins are synthesized in the ER, where folding and the initial stages of glycosylation (high-mannose type glycans) occur. They are then targeted to lysosomes via the trans-Golgi network, acquiring further modifications (complex type N-glycans). To verify the glycosylation stage of WT cystinosin and ΔITILELP, we performed enzymatic deglycosylation using the peptide:N-glycosidase F enzyme (PNGase F), which removes all *N*-linked glycan residues. As a control, we used N1N7, the constitutively deglycosylated form of cystinosin. After incubation with PNGase F, WT cystinosin had the migration profile of N1N7, while N1N7 did not show any changes (Figure 7A), showing that WT cystinosin is indeed heavily glycosylated. ΔITILELP was also completely deglycosylated by PNGase F, showing that it also contains a certain level of glycosylation. N288K and N323K, used as positive controls, showed the same electrophoretic profile as WT cystinosin.

We therefore tested the effect of the Endoglycosidase H enzyme (Endo H), as it specifically hydrolyses non-mature N-glycans (high-mannose type). In contrast to WT cystinosin, ΔITILELP was sensitive to Endo H digestion (Figure 7B), suggesting that ΔITILELP carries high-mannose on its available glycosylation sites. WT cystinosin is not affected by Endo H digestion, confirming that the WT form contains complex-type glycans, acquired during maturation in the Golgi apparatus.

DISCUSSION

ASBMB MOLECULAR & CELLULAR PROTEOMICS MCP

In this study, we investigated the impact of cystinosin deletion ΔITILELP on the stability of the protein. The ΔITILELP mutation disrupts the proper glycosylation of cystinosin on N66. In the homozygous state, ΔITILELP leads to juvenile cystinosis, which correlates with the ability to maintain minimal cystine transport activity *in vitro* (9). However, when found in the heterozygous state together with a 57 kb deletion on the second allele, the ΔITILELP mutation can result in the development of the severe infantile phenotype (7, 8). These surprising observations led us to hypothesize that the deletion of seven amino acids, together with the lack of glycosylation on N66, interferes with cystinosin stability.

To investigate ΔITILELP turnover, we used the dynamic SILAC approach with MS. However, we faced two main challenges. First, cystinosin is not easily detectable by MS in non-fractionated samples, such as a total cell lysate or blood (no records on peptide identification in proteomic studies are reported at nextprot.org). This is probably due to the very low abundance of endogenous cystinosin in cells and to characteristics of its sequence, which contains seven TM domains and seven glycosylation sites. To our knowledge, endogenous cystinosin was identified with two peptides in only one MS study of enriched lysosomal membranes (23). Furthermore, no good antibodies are available to immunoprecipitate endogenous cystinosin from cell lysates in order to enrich endogenous cystinosin. For these reasons, we developed cellular models of stably expressing EGFP-tagged WT and mutated cystinosin. Although these tagged proteins localize correctly in the lysosome and have been previously used for functional studies, we are aware that the use of EGFP-tagged cystinosin is a constraint and we cannot be certain that the endogenous proteins follow exactly the same behaviour. In this study, we detected four peptides of cystinosin (two from WT cystinosin and two specific to mutants) and provided evidence that the N-terminal signal peptide can be cleaved before S23.

The second challenge was that dynamic SILAC, although a well-established approach, can be tricky when studying the turnover of stable proteins. We calculated the K_{loss} from the MS1 areas of the peptides and

ASBMB MOLECULAR & CELLULAR PROTEOMICS MCP

their labelled counterparts using curve-fitting or mathematical formulas applied to each time-point (reported in different forms in the literature, but equivalent) (14, 16). Our data confirmed that the K_{loss} values calculated by curve-fitting and mathematical formulas correlate perfectly when many data points are used in the calculations. However, stable proteins such as WT cystinosin are virtually undegraded during the cell cycle/lifespan (rate of degradation: K_{deg}), and are only diluted upon cell division. In this case, the rate of loss (K_{loss}) of the protein is very close to the cell-division rate (D), and the $K_{deg}=K_{loss}-D$ value nearly reaches zero. After verifying that D was similar for all of the cell lines studied, we chose to report and compare the K_{loss} of WT cystinosin and the mutants.

Our dynamic SILAC data showed that WT cystinosin is a very stable protein and that the ΔITILELP mutation increased three-fold the degradation of the protein, while the N288K and N323K mutations did not significantly influence the protein's stability. We clearly showed that ΔITILELP undergoes lysosomal degradation, as v-ATPase inhibition by bafilomycin A1 (BafA1), but not proteasomal inhibition, resulted in increased cellular levels as observed by an increased fluorescence signal. The rate of lysosomal degradation of ΔITILELP was three times greater than that of the WT protein, further confirming the instability of this mutant.

We have recently demonstrated that cystinosin mutations, in addition to inefficient efflux of cystine from the lysosome, induce changes in the protein network that might modulate the role of cystinosin in the mTOR pathway (5). For this reason, we decided to investigate the ΔITILELP protein network. Our interactomic study revealed that similar to WT cystinosin, ΔITILELP maintains interactions at the lysosomal membrane with the V-ATPase complex and some proteins of the mTOR pathway. The presence of functional ΔITILELP on the lysosomal membrane aligns with the fact that patients with homozygous ΔITILELP mutations develop juvenile rather than infantile cystinosis. In addition, ΔITILELP interacts with 15 proteins of the ER, most of which have been implicated in ER quality-control and

ASBMB MOLECULAR & CELLULAR PROTEOMICS MCP

processing (e.g. calreticulin, Os9, Sel1l) (24). Immunofluorescence studies confirmed these findings and showed the partial localization of ΔITILELP in the ER and in lysosomes.

The accumulation of misfolded proteins in the ER can lead to ER stress and cell death. To prevent cell injury, non-native proteins can exit the ER to undergo proteasomal and/or lysosomal degradation (25, 26). To better understand the reasons for ER retention, we further explored the extent of the faulty glycosylation of ΔITILELP and demonstrated that it carried immature high-mannose glycans in all six remaining sites not directly affected by the mutation, suggesting that it is prevented from reaching the Golgi network for further processing. This is coherent with the observed ΔITILELP molecular weight by SDS-PAGE. Several studies have been conducted to decipher the glyco-code of processed proteins, revealing the importance of N-glycans in directing protein maturation (27). The glycan composition controls the calnexin binding cycle, which is important for the recognition of misfolded proteins in the ER (28, 29). Along these lines, the strong interaction shown in our study between ΔITILELP and the ER chaperone, calnexin, suggested that this mutant was recognized as a non-native protein by the ER quality-control system and was partially retained in this compartment. The N1N7 mutant, which does not carry any glycosylation, is correctly directed from the ER to the lysosome and its stability is not affected.

We suggest that ΔITILELP is initially retained in the ER, preventing it from being processed in the Golgi to obtain mature glycosylation, but it is directly transported to lysosome via its two targeting sequences. Further studies will be necessary to fully understand the escape mechanisms of ΔITILELP from the ER to the lysosome. One possible mechanism is ER macro-autophagy that may be induced by ER stress (30). However, some unconventional cellular mechanisms of ER escape by retained proteins have also been described. Non-mature CFTR can be targeted to the plasma membrane, skipping the Golgi compartment via the unconventional GRASP-dependent pathway (31). Additionally, the formation of ER-derived

ASBMB MOLECULAR & CELLULAR PROTEOMICS MCP

vesicles referred to as EDEMosomes, which are necessary for ERAD tuning, enable the removal of selected ERAD regulators from the ER and their degradation by proteasomes and endolysosomal proteases. These vesicles contain EDEM1 and Sel1L but can also carry other ER proteins (32).

We conclude that the high turnover of ΔITILELP, due to its immature glycosylation state together with low transport activity, might be responsible for the phenotype observed in some patients who carry this mutation heterozygously, together with the 57 kb deletion.

ACKNOWLEDGMENTS

We greatly appreciate Prof. R.J. Beynon for valuable advice in turnover data interpretation, Dr. P. Codogno and Dr. A. Delaunay-Moisan for thoughtful discussions, N. Gaudin, M. Garfa-Traore, and R. Desvaux at Imagine Cell Imaging for expert assistance in confocal microscopy.

FUNDING

This work was supported by grants from the Cystinosis Research Foundation and from the Investments for the Future program (ANR-10-IAHU-01).

ASBMB MOLECULAR & CELLULAR PROTEOMICS MCP

REFERENCES

1. Gahl, W. A., Thoene, J. G., and Schneider, J. A. (2002) Cystinosis. *N. Engl. J. Med.* 347, 111–121

2. Town, M., Jean, G., Cherqui, S., Attard, M., Forestier, L., Whitmore, S. A., Callen, D. F., Gribouval, O., Broyer, M., Bates, G. P., van't Hoff, W., and Antignac, C. (1998) A novel gene encoding an integral membrane protein is mutated in nephropathic cystinosis. *Nat. Genet.* 18, 319–324

3. Cherqui, S., Kalatzis, V., Trugnan, G., and Antignac, C. (2001) The targeting of cystinosin to the lysosomal membrane requires a tyrosine-based signal and a novel sorting motif. *J. Biol. Chem.* 276, 13314–13321

4. Kalatzis, V., Cherqui, S., Antignac, C., and Gasnier, B. (2001) Cystinosin, the protein defective in cystinosis, is a H(+)-driven lysosomal cystine transporter. *EMBO J.* 20, 5940–5949

5. Andrzejewska, Z., Nevo, N., Thomas, L., Chhuon, C., Bailleux, A., Chauvet, V., Courtoy, P. J., Chol, M., Guerrera, I. C., and Antignac, C. (2015) Cystinosin is a Component of the Vacuolar H+-ATPase-Ragulator-Rag Complex Controlling Mammalian Target of Rapamycin Complex 1 Signaling. *J. Am. Soc. Nephrol.* 27, 1678-1688.

6. Andrzejewska, Z., Névo, N., Thomas, L., Bailleux, A., Chauvet, V., Benmerah, A., and Antignac, C. (2015) Lysosomal Targeting of Cystinosin Requires AP-3. *Traffic* 16, 712–726

7. Heil, S. G., Levtchenko, E., Monnens, L. A., Trijbels, F. J., Van der Put, N. M., and Blom, H. J. (2001) The molecular basis of Dutch infantile nephropathic cystinosis. *Nephron.* 89, 50–55

8. Kalatzis, V., Nevo, N., Cherqui, S., Gasnier, B., and Antignac, C. (2004) Molecular pathogenesis of cystinosis: effect of CTNS mutations on the transport activity and subcellular localization of cystinosin. *Hum. Mol. Genet.* 13, 1361–1371

9. Midgley, J. P., El-Kares, R., Mathieu, F., and Goodyer, P. (2011) Natural history of adolescent-onset cystinosis. *Pediatr. Nephrol.* 26, 1335–1337

10. Marshall, R. D. (1972) Glycoproteins. *Annu. Rev. Biochem.* 41, 673–702

11. Kundra, R., and Kornfeld, S. (1999) Asparagine-linked oligosaccharides protect Lamp-1 and Lamp-2 from intracellular proteolysis. *J. Biol. Chem.* 274, 31039–31046

12. Doherty, M. K., Hammond, D. E., Clague, M. J., Gaskell, S. J., and Beynon, R. J. (2009) Turnover of the human proteome: determination of protein intracellular stability by dynamic SILAC. *J. Proteome Res.* 8, 104–112

13. Beynon, R. J. (2005) The dynamics of the proteome: strategies for measuring protein turnover on a proteome-wide scale. *Brief Funct. Genomic Proteomic* 3, 382–390

14. Schwanhäusser, B., Busse, D., Li, N., Dittmar, G., Schuchhardt, J., Wolf, J., Chen, W., and Selbach, M. (2011) Global quantification of mammalian gene expression control. *Nature* 473, 337–342

ASBMB MOLECULAR & CELLULAR PROTEOMICS MCP

15. Zufferey, R., Donello, J. E., Trono, D., and Hope, T. J. (1999) Woodchuck hepatitis virus posttranscriptional regulatory element enhances expression of transgenes delivered by retroviral vectors. *J. Virol.* 73, 2886–2892

16. Pratt, J. M., Petty, J., Riba-Garcia, I., Robertson, D. H. L., Gaskell, S. J., Oliver, S. G., and Beynon, R. J. (2002) Dynamics of protein turnover, a missing dimension in proteomics. *Mol. Cell Proteomics* 1, 579–591

17. Vizcaíno, J. A., Csordas, A., del-Toro, N., Dianes, J. A., Griss, J., Lavidas, I., Mayer, G., Perez-Riverol, Y., Reisinger, F., Ternent, T., Xu, Q.-W., Wang, R., and Hermjakob, H. (2016) 2016 update of the PRIDE database and its related tools. *Nucleic Acids Res.* 44, D447–D456

18. Cox, J., and Mann, M. (2008) MaxQuant enables high peptide identification rates, individualized p.p.b.-range mass accuracies and proteome-wide protein quantification. *Nat. Biotechnol.* 26, 1367–1372

19. Cox, J., Hein, M. Y., Luber, C. A., Paron, I., Nagaraj, N., and Mann, M. (2014) MaxLFQ allows accurate proteome-wide label-free quantification by delayed normalization and maximal peptide ratio extraction. *Mol. Cell Proteomics* mcp.M113.031591

20. Tyanova, S., Temu, T., Sinitcyn, P., Carlson, A., Hein, M. Y., Geiger, T., Mann, M., and Cox, J. (2016) The Perseus computational platform for comprehensive analysis of (prote)omics data. *Nat. Meth.* 13, 731–740

21. Attard, M., Jean, G., Forestier, L., Cherqui, S., van't Hoff, W., Broyer, M., Antignac, C., and Town, M. (1999) Severity of phenotype in cystinosis varies with mutations in the CTNS gene: predicted effect on the model of cystinosin. *Hum. Mol. Genet.* 8, 2507–2514

22. Lamriben, L., Graham, J. B., Adams, B. M., and Hebert, D. N. (2016) N-Glycan-based ER Molecular Chaperone and Protein Quality Control System: The Calnexin Binding Cycle. *Traffic* 17, 308–326

23. Schröder, B., Wrocklage, C., Pan, C., Jäger, R., Kösters, B., Schäfer, H., Elsässer, H.-P., Mann, M., and Hasilik, A. (2007) Integral and Associated Lysosomal Membrane Proteins. *Traffic* 8, 1676–1686

24. Bernasconi, R., Galli, C., Calanca, V., Nakajima, T., and Molinari, M. (2010) Stringent requirement for HRD1, SEL1L, and OS-9/XTP3-B for disposal of ERAD-LS substrates. *J. Cell Biol.* 188, 223–235

25. Chiang, W.-C., Messah, C., and Lin, J. H. (2012) IRE1 directs proteasomal and lysosomal degradation of misfolded rhodopsin. *Mol. Biol. Cell* 23, 758

26. Dersh, D., Jones, S. M., Eletto, D., Christianson, J. C., and Argon, Y. (2014) OS-9 facilitates turnover of nonnative GRP94 marked by hyperglycosylation. *Mol. Biol. Cell* 25, 2220–2234

27. Hebert, D. N., Lamriben, L., Powers, E. T., and Kelly, J. W. (2014) The intrinsic and extrinsic effects of N-linked glycans on glycoproteostasis. *Nat. Chem. Biol.* 10, 902

28. Hammond, C., Braakman, I., and Helenius, A. (1994) Role of N-linked oligosaccharide recognition, glucose trimming, and calnexin in glycoprotein folding and quality control. *Proc. Natl. Acad. Sci. U. S. A.* 91, 913

ASBMB MOLECULAR & CELLULAR PROTEOMICS MCP

29. Helenius, A. (1994) How N-linked oligosaccharides affect glycoprotein folding in the endoplasmic reticulum. *Mol. Biol. Cell* 5, 253–265

30. Høyer-Hansen, M., and Jäättelä, M. (2007) Connecting endoplasmic reticulum stress to autophagy by unfolded protein response and calcium. *Cell Death & Differentiation* 14, 1576–1582

31. Gee, H. Y., Noh, S. H., Tang, B. L., Kim, K. H., and Lee, M. G. (2011) Rescue of ΔF508-CFTR Trafficking via a GRASP-Dependent Unconventional Secretion Pathway. *Cell* 146, 746–760

32. Bernasconi, R., and Molinari, M. (2011) ERAD and ERAD tuning: disposal of cargo and of ERAD regulators from the mammalian ER. *Curr. Opin. Cell Biol.* 23, 176–183

ASBMB MOLECULAR & CELLULAR PROTEOMICS MCP

FIGURE LEGENDS

Figure 1. Protein topology plot and electrophoretic profiles of WT cystinosin and ΔITILELP. (A) Cystinosin and (B) ΔITILELP are schematically represented with their theoretical tryptic sites obtained by PeptideMass software (red dash) and detected peptides obtained by Q-Exactive Orbitrap (red circle). (C) Lysates of NIH/3T3 cells expressing cystinosin-EGFP, N66A (single N-glycosylation site-deleted mutant) and ΔITILELP were resolved by SDS-PAGE on 10% gel, then analyzed by immunoblotting with anti-GFP antibody.

Figure 2. MS1 areas of peptide FSVSGEGEGDATYGK in EGFP-tagged cystinosin, ΔITILELP, N288K and N323K. The peaks correspond to the extracted ion chromatogram of the MS1 signal of the pre-existing peptides in the course of degradation (red trace, light label) and the newly synthetized peptides (blue trace, heavy label). The MS1 areas were extracted and represented using Skyline software for all time-points.

Figure 3. Degradation curves of cystinosin and its mutants. RIA (relative isotope abundance, *y* axis) for each time point (*x* axis) were plotted using GraphPad software. The curve in black represents the degradation of WT cystinosin, while the curve in red represents the degradation curve of the indicated mutant. The histograms represent the loss rate (K_{loss}) for each protein and its two components: rate of degradation (K_{deg}) and cell-division rate (D).

Figure 4. Lysosomal degradation pathway of cystinosin. NIH/3T3 cells stably expressing cystinosin-EGFP or ΔITILELP-EGFP were treated for 24 h with the proteasome inhibitor clasto-lactacystin (CL), with the lysosomal inhibitor bafilomycin A1 (Baf A1), or with DMSO as the vehicle control. Fluorescence intensity was determined by flow cytometry. Quantification of EGFP-fusion protein levels is represented as fluorescence intensity (*** $p<0.0001$ as compared to the control; each bar represents mean ± SEM of five experiments). Representative FACS profiles are shown.

ASBMB MOLECULAR & CELLULAR PROTEOMICS MCP

Figure 5. Protein partners for WT cystinosin and ΔITILELP in lysosomal and reticular compartments. Volcano plot representation of proteins immunoprecipitated by the anti-GFP antibody and identified by mass spectrometry in ΔITILELP-EGFP- *vs* cystinosin-EGFP-expressing cells. In blue, proteins known to be lysosomal partners of cystinosin. In red, proteins classified by the KEGG pathway database as "protein processing in endoplasmic reticulum".

Figure 6. ER retention of ΔITILELP. (A) NIH/3T3 cell lines stably expressing cystinosin-EGFP, ΔITILELP, N288K and N323K were co-labelled for PDI or Lamp-1 (confocal microscopy; scale bars=10 µm). These images are representative of three biological replicates. (B) Targeting of cystinosin-EGFP (WT and mutants), quantified as the percentage of the protein that is positive for PDI or Lamp-1 within five cells per group. The percentage of colocalization between cystinosin-EGFP and PDI or Lamp-1 was analyzed with the ImageJ 1.50 software (** $p<0.005$, *** $p<0.0001$ as compared to WT cystinosin). (C) NIH/3T3 cell lines stably expressing cystinosin-EGFP, ΔITILELP, N288K and N323K were immunoprecipitated with anti-GFP antibody, and co-immunoprecipitated calnexin was analyzed by western-blotting. Representative blots from four independent experiments are shown. (D) Quantification of the calnexin signal normalized to the cystinosin signal (WT and mutants) (* $p<0.05$ as compared to WT cystinosin; each bar represents mean ± SEM from four independent experiments).

Figure 7. Deglycosylation of cystinosin and its mutated forms. (A) Lysates of NIH/3T3 cell lines stably expressing cystinosin-EGFP, N1N7 (seven N-glycosylation site-deleted mutants), ΔITILELP, N288K and N323K were incubated with or without PNGase F for 1 h at 37°C to remove N-glycans. (B) Lysates of NIH/3T3 cell lines stably expressing cystinosin-EGFP and ΔITILELP were incubated with or without Endo H for 1 h at 37°C to cleave specifically immature N-glycans. All lysates were resolved by SDS-PAGE on 10% gel and analyzed by immunoblotting with anti-GFP antibody.

ASBMB
MOLECULAR & CELLULAR PROTEOMICS
MCP

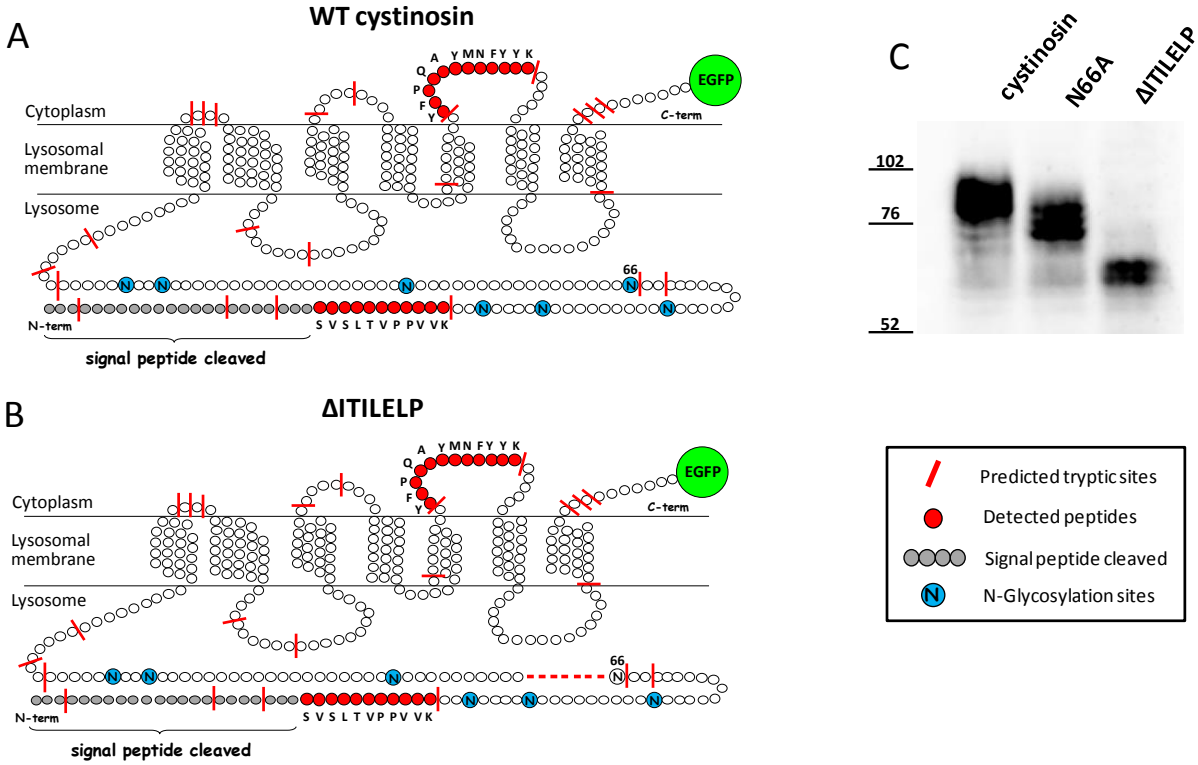

Figure 1

ASBMB
MOLECULAR & CELLULAR PROTEOMICS
MCP

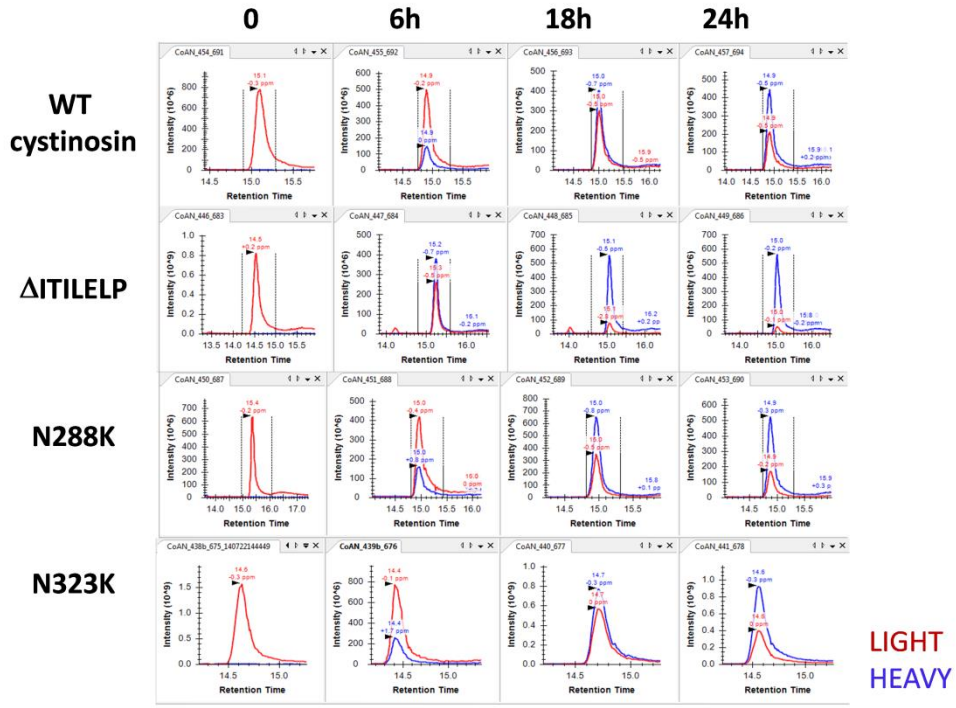

Figure 2.

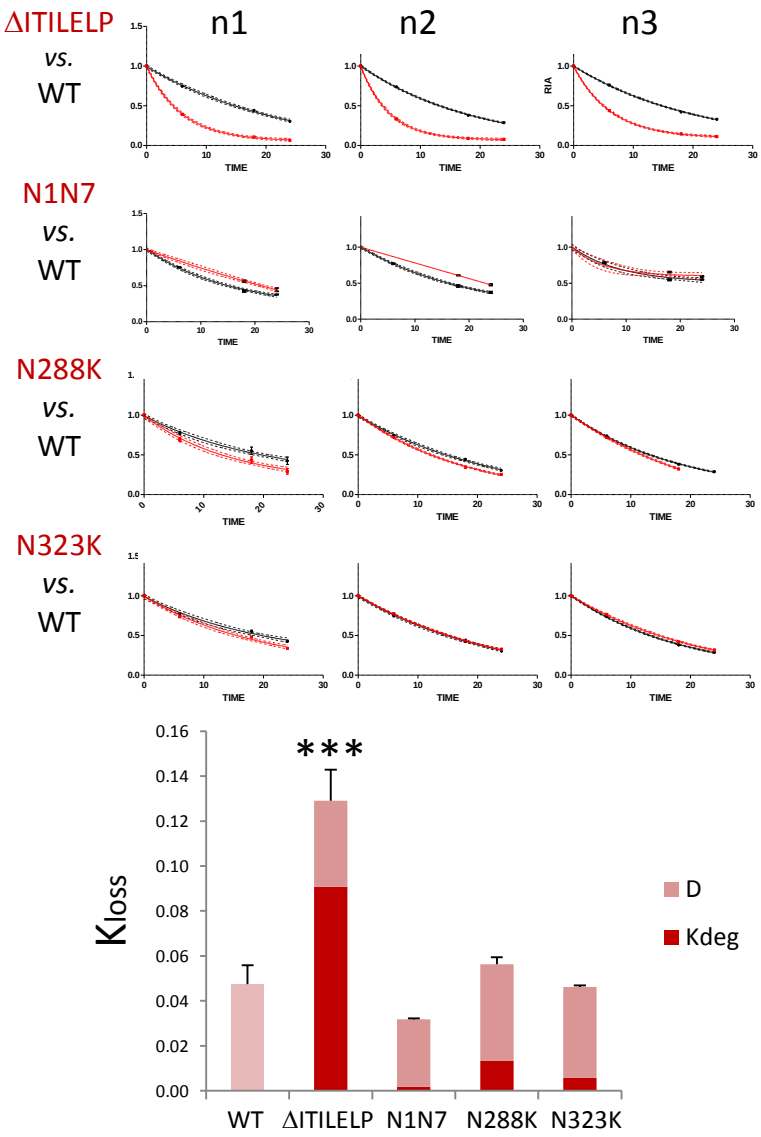

Figure 3

ASBMB
MOLECULAR & CELLULAR PROTEOMICS
MCP

ASBMB
MOLECULAR & CELLULAR PROTEOMICS
MCP

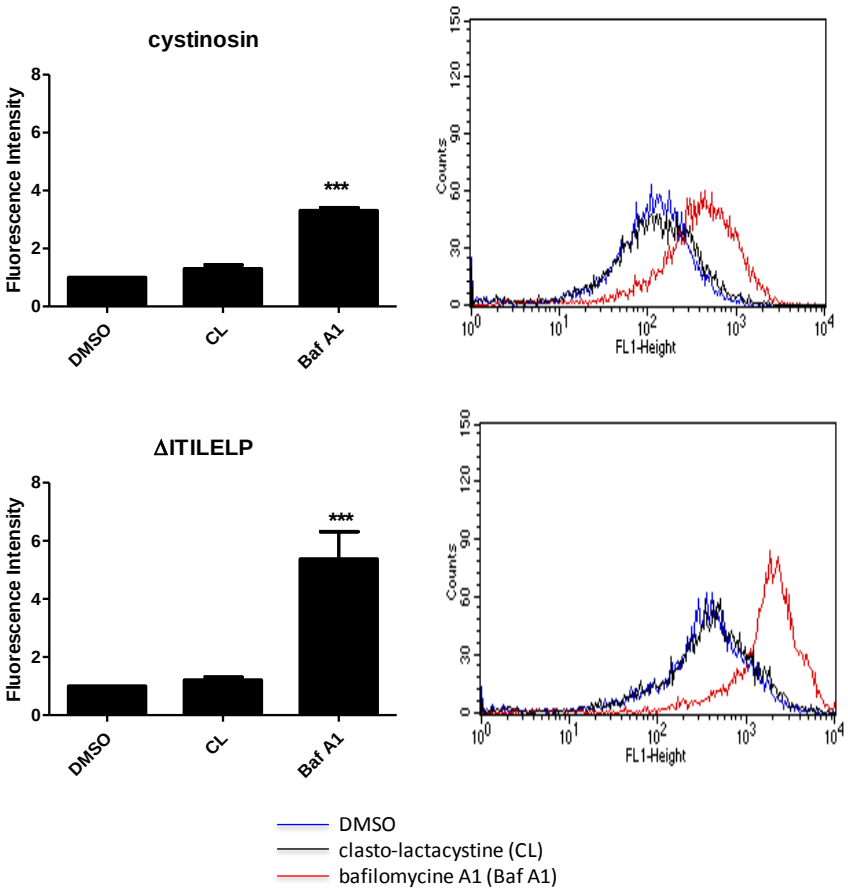

Figure 4

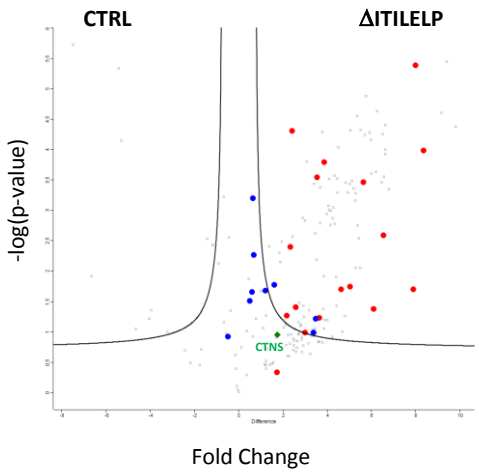

	Protein names	Gene names
Lysosomal partners	V-type proton ATPase subunit D	Atp6v1d
	V-type proton ATPase subunit C 1	Atp6v1c1
	V-type proton ATPase subunit E 1	Atp6v1e1
	V-type proton ATPase subunit B, brain isoform	Atp6v1b2
	V-type proton ATPase catalytic subunit A	Atp6v1a
	V-type proton ATPase 116 kDa subunit a isoform 1	Atp6v0a1
	V-type proton ATPase subunit G 1	Atp6v1g1
	V-type proton ATPase subunit H	Atp6v1h
	Ras-related GTP-binding protein C	Rragc
ER partners	Protein sel-1 homolog 1	Sel1l
	Peptide-N(4)-(N-acetyl-beta-glucosaminyl)asparagine amidase	Ngly1
	Protein OS-9	Os9
	Translocon-associated protein subunit delta	Ssr4
	S-phase kinase-associated protein 1	Skp1
	E3 ubiquitin-protein ligase AMFR	Amfr
	Cullin-1	Cul1
	F-box only protein 6	Fbxo6
	Endoplasmic reticulum lectin 1	Erlec1
	Glycosyltransferase STT3A	Stt3a
	Phospholipase A-2-activating protein	Plaa
	Protein disulfide-isomerase A6	Pdia6
	Glycosyltransferase STT3B	Stt3b
	Calnexin	Canx
	Derlin-2	Derl2
	Translocon-associated protein subunit alpha	Ssr1
	Calreticulin	Calr

Figure 5

ASBMB MOLECULAR & CELLULAR PROTEOMICS MCP

ASBMB
MOLECULAR & CELLULAR PROTEOMICS
MCP

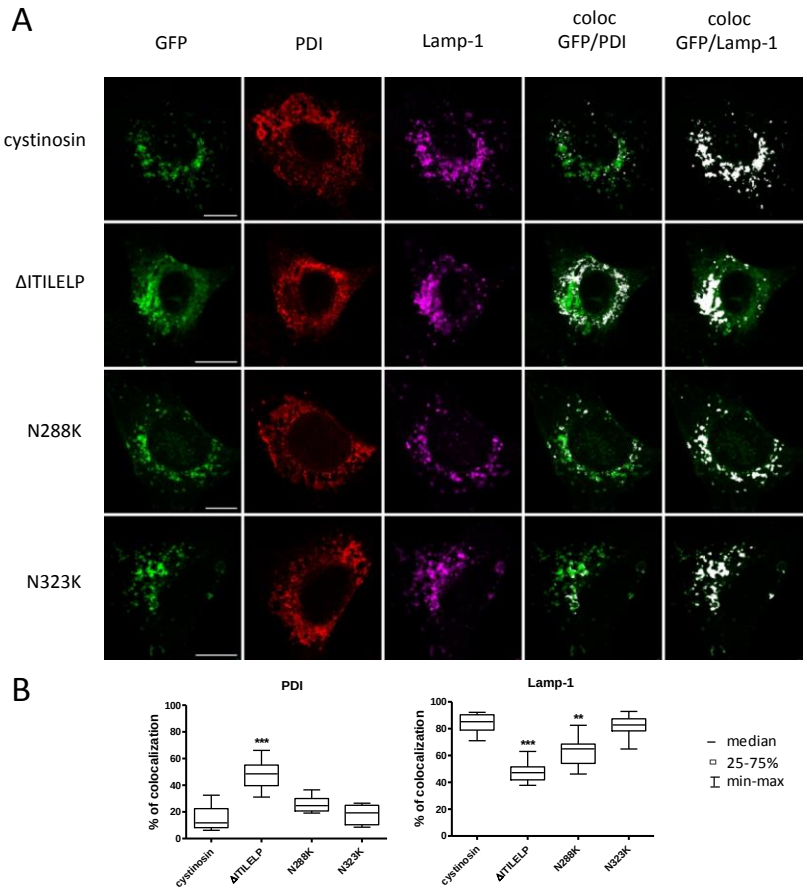

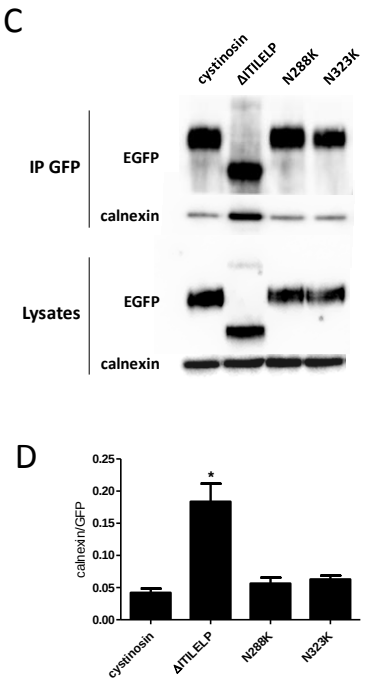

Figure 6.

Figure 6

ASBMB
MOLECULAR & CELLULAR PROTEOMICS
MCP

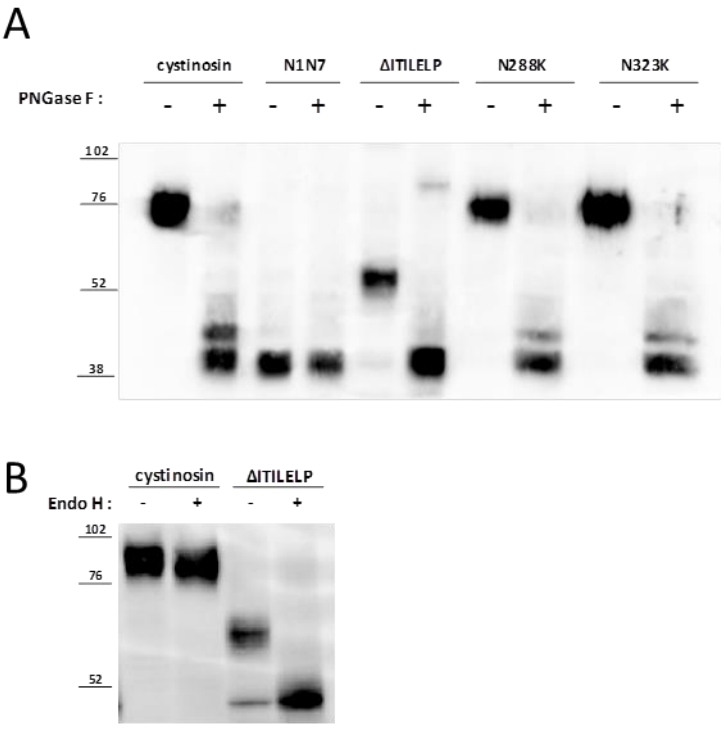

Figure 7